

1 **Comparing electronic probes for volumetric water content of low-density**  
2 **feathermoss.**

3

4

5 Pier P. Overduin, Kenji Yoshikawa, Douglas L. Kane, Jennifer W. Harden

6

7 P. P. Overduin, K. Yoshikawa, and D. L. Kane, Water and Environmental Research  
8 Center, Institute of Northern Engineering, University of Alaska Fairbanks, P.O. Box  
9 755860, Fairbanks, Alaska 99775-5860, USA.

10 J. W. Harden, U.S. Geological Survey, 345 Middlefield Rd., MS 962, Menlo Park, CA  
11 94025, USA.

12

12 **ABSTRACT**

13 Feathermoss is ubiquitous in the boreal forest and across various land-cover types of the  
14 arctic and sub arctic. A variety of affordable commercial sensors for soil moisture content  
15 measurement have recently become available and are in use in such regions, often in  
16 conjunction with fire-susceptibility or ecological studies. Electromagnetic sensors  
17 available include frequency and time domain designs with variations in wave guide and  
18 sensor geometry, the location of sensor electronics and operating frequency. Few come  
19 supplied with calibrations suitable or suggested for low bulk density soils high in  
20 organics. We tested seven of these sensors (CS615, ECH2O, GroPoint, Vitel, Theta,  
21 TDR, Watermark) for use in feathermoss. Sensors installed in live, dead and burned  
22 feathermoss samples, drying in a controlled manner, were monitored continuously and  
23 compared to gravimetric determinations of moisture content. Almost all of the sensors  
24 tested were suitable for measuring the moss sample water content over a range of water  
25 contents from dry to field capacity, and we present a unique empirical calibration for each  
26 sensor for this material. Differences in sensor design lead to changes in sensitivity as a  
27 function of volumetric water content. These differences will affect the spatial averaging  
28 over the soil measurement volume. Sensitivity analysis shows that empirical calibrations  
29 are required for different soil types.

## 30 INTRODUCTION

### 31 1.1 *Electromagnetic Techniques for Measuring Volumetric Water Content*

32 Since the 1960s, electromagnetic techniques have been studied and used for measuring  
33 the volumetric water content of porous media. Most applications in the geosciences have  
34 been in mineral soils, for which both empirical relationships (for example, Ledieu et al.,  
35 1986; Topp et al.; 1980, Stein and Kane 1983) and theoretical models (for example, Roth  
36 et al., 1990) exist for estimating volumetric water content from the bulk relative dielectric  
37 permittivity. A few empirical relationships exist for soils high in organic content  
38 (Herkelrath et al., 1991; Roth et al., 1992), but not for mosses other than cultivated peat  
39 derived from *Sphagnum* moss (Myllys and Simojoki 1996). Based on their review of  
40 calibration equations, Jacobsen and Schønning (1995) suggested that organic soils might  
41 require special treatment.

42 Under the assumption that all moss tissue has a common dielectric constant,  
43 differences in the bulk dielectric constant of mosses at the same volumetric water content  
44 are due to differences in volumetric fractions of air and moss in the sampling volume, i.e.  
45 to differences in bulk density and to differences in the distribution of water between  
46 bound and free states. Moss differs from low bulk density soils in that the solid phase is  
47 composed mostly of organics with highly polar surfaces and a significant portion of the  
48 soil water is incorporated into the moss as inner-cellular solution, which may have a  
49 different dielectric constant than that of free water. Both factors can be expected to  
50 increase the proportion of water in a bound state relative to mineral soils with similar  
51 characteristic particle size and therefore to decrease the apparent relative dielectric  
52 permittivity of the bulk soil for a similar water content.

53            Assuming a representative volume element of soil, a general relationship between  
54 the real part of the dielectric permittivity,  $\phi$ , and the volumetric water content,  $\theta$ , should  
55 exist for a porous medium with spatially homogeneous composition, porosity and texture.  
56 In practice, however, the apparent relative dielectric permittivity of the medium is also  
57 affected by sensor measurement frequency and geometry and medium structure, density,  
58 and water content (Topp et al., 1980). An empirical calibration lumps together the  
59 influences of the medium and of the sensor on the measurement. Most calibrations  
60 presented in the literature deviate from Topp's relationship (Topp et al., 1980; for  
61 example, Jacobsen and Schønning, 1995) and soil texture is generally invoked as the  
62 cause of the deviation. Attempts have been made to extend the applicability of TDR  
63 calibration curves by soil characteristics such as bulk density (e.g. Malicki, 1989). In  
64 practice, this will not eliminate the necessity of sampling the material, or similar  
65 materials, in which water content measurements are to be carried out in order to create  
66 suitable calibration curves.

67            More than 23 studies of the TDR technique in a wide variety of materials are  
68 available in the literature. Third-order calibration curves for peat moss, litter or soils high  
69 in organic or measured carbon content are available from Herkelrath et al., (1991),  
70 Ledieu et al., (1986), Myllys and Simojoki (1996), Pepin et al., (1992), Roth et al.,  
71 (1992), and Topp et al., (1980). Mineral soil calibrations (e.g. Dasberg and Hopmans,  
72 1992; Jacobsen and Schønning, 1995; Ledieu et al., 1986; Malicki and Skierucha, 1989;  
73 Nadler et al., 1991) predict higher relative dielectric permittivities for volumetric water  
74 contents above  $0.4 \text{ m}^3 \text{ m}^{-3}$ , consistent with the prediction made above. Below this value,  
75 the regions bounded by organic and mineral calibrations overlap.

76           Sensor type influences the calibration through sensor geometry and frequency,  
77 both of which affect the spatial weighting function applied to the soil volume (Ferré et al,  
78 1996; Nissen et al., 2003; Zegelin et al., 1989). Both the measurement volume and spatial  
79 weighting are dependent on sensor design (Ferré et al., 1996; Knight 1992; Zegelin et al.,  
80 1989; Pepin et al., 1992). Ferré et al (1996) showed that sensor output averages variations  
81 in water content along the wave guides for uncoated wave guides but not for coated wave  
82 guides. For all sensor designs, the soil volume proximal to the sensor wave guides is  
83 more heavily weighted in averaging of the apparent relative dielectric permittivity. Thus,  
84 the density of plant tissue immediately adjacent to the tines of the sensor exerts a  
85 disproportionately large influence on sensor output. Thicker tined-sensors, which shift  
86 and compact more of the solid soil matrix (moss tissue) on insertion may have a tendency  
87 to change the character of this near-tine material to a greater degree, particularly in a low  
88 bulk-density material.

89           Since TDR was developed and gained common usage as a means of measuring  
90 volumetric soil water, numerous other devices exploiting the sensitivity of the relative  
91 dielectric permittivity to soil water content have appeared on the market. They have the  
92 advantage of being cheaper and simpler to employ than TDR. While TDR measurements  
93 are only slightly influenced by the nature of the soil (Ledieu et al., 1986), most  
94 inexpensive commercially available sensors, both time domain and capacitance, provide  
95 calibrations relating sensor output directly to volumetric water content for use in a limited  
96 number of media. As with the empirical relationships in the literature, none provide  
97 calibrations with a finer distinction than mineral vs. organic soils.

98 Feathermoss is virtually ubiquitous in the boreal forest and common in higher  
99 latitudes. Its presence is sensitive to changes in environmental conditions and particularly  
100 to changes in water content. The water content of moss cover in both of these regions is  
101 also important because it determines boreal forest fire susceptibility, and because the  
102 thermal properties of the surface layers are highly sensitive to water levels (Yoshikawa et  
103 al., 2003). The bulk thermal conductivity and heat capacity of this surface layer have  
104 been shown elsewhere to play a pivotal role in controlling permafrost persistence or  
105 degradation (Yoshikawa et al., 2003).

106 Feather mosses include species from a number of genera, all of which share  
107 similar morphological characteristics, such as prostrate growth habit and branched stems.  
108 Dry bulk densities for feathermoss species have been reported in the literature (Table 1)  
109 and cover a range from 0.01 to 0.05 kg m<sup>-3</sup>. Feathermoss changes in bulk density within  
110 live and decomposing layers, as well as generally over depth. As an indication of their  
111 variability, values for dry bulk density from a number of sources are plotted with sample  
112 depth in Figure 1. Higher dry bulk densities are recorded with greater depth, and reflect  
113 the accumulation of dead moss tissue beneath the living layer.

114 In this paper, we test the suitability of a number of electromagnetic devices for  
115 measuring the volumetric water content of feathermoss. These sensors are used in  
116 feathermoss in Arctic (Romanovsky and Osterkamp, 2000; Hinkel et al., 2001) and sub-  
117 Arctic (Harden et al., 2004) soils. The differences between sensor calibrations and the  
118 influence of their design are important considerations when planning field measurements  
119 and when comparing data derived from different sensors or sensors measuring water  
120 content in differing materials. This has particular relevance to climate gradient and

121 remote-sensing studies that seek to compare results from different ecosystems or to  
122 ground-truth spatially distributed data.

## 123 **METHODS**

124 Seven electronic sensors were tested and included two time domain reflectometry  
125 sensors: the TDR100 (Campbell Scientific, Inc.) with the CS605 TDR probe and the  
126 GroPoint (Environmental Sensors Inc.). Four capacitance (sometimes referred to as  
127 frequency domain reflectometry or FDR) sensors were also included: the CS615 probe  
128 (Campbell Scientific, Inc.), the ECH<sub>2</sub>O probe (Decagon device, Inc.), the Hydra Vitel  
129 probe (Stevens Water Monitoring Systems Inc.), and the Theta ML2x Delta-T probe  
130 (Delta-T devices, Inc.), as well as a device based on measured electrical resistance, the  
131 Watermark sensor model 200SS (Irrometer Co.). Other than the latter device, each sensor  
132 has unique wave-guide geometry, frequency and electronics, details of which are given in  
133 Table 2. The CS615, ECH<sub>2</sub>O, GroPoint, Hydra Vitel probe, Theta probe and carry on-  
134 board electronics, while the TDR probe is a simple wave-guide. The wave-guide  
135 geometry is important for the ease of installation, disturbs the soil matrix on installation  
136 to different degrees and changes the soil volume over which the measurement is made.  
137 Finally, the ECH<sub>2</sub>O probe is unique among the electromagnetic sensors tested here,  
138 because its tines are encased in a sensor board.

139         Methods were selected to demonstrate that the seven soil water sensors listed in  
140 Table 2 were effective in determining the water content of the live and dead part of  
141 feathermoss. Bulk samples of forest floor feathermoss were harvested in spring (May and  
142 June) from three locations around Fairbanks, Alaska (Birch Hill, University Ski Trails  
143 and Delta Junction). Each block contained a mix of feathermoss species, in each case

144 predominantly of *Pleurozium* and *Hylocomium* species. Both live and decomposing moss  
145 was collected in each case. A sample of burned, partially charred moss from the Tanana  
146 River flood plain, Alaska was also used for TDR calibration. The four feathermoss  
147 samples were discriminated by layer (live or dead) and cut to known volume. Live and  
148 dead moss layers are usually distinguished on the basis of color, the presence of litter and  
149 the relative proportion of fibric moss tissue. In practice, we found a division of lesser  
150 cohesion between more loosely bound live moss tissue and the underlying, more tightly  
151 matted dead moss tissue, which roughly corresponded to the division based on color.  
152 Each layer was over 0.1 m thick.

153         The seven sensors were placed in the sample block in parallel orientation,  
154 extending from the insertion side of the block into its interior. Feathermoss sample blocks  
155 were set in an upright position and allowed to soak for more than 24 hours before  
156 measurements began. The saturated feathermoss samples, including sensors, were lifted  
157 out of the water in mesh baskets, drained to approximately field capacity and weighed  
158 during drying in a 30°C forced air oven using an electronic balance. Sensor cables were  
159 supported to avoid their influence on the measured weight and the sensors remained  
160 inserted in the samples for the duration of the experiment. Balance output was recorded  
161 every 5 minutes. Temperature data within the oven and the moss samples was recorded  
162 using thermistors at 5-minute intervals during the experiment. Sensor output was  
163 measured simultaneously with all seven sensors at five-minute intervals during drying  
164 until the sample block reached a stable weight over a twelve-hour period. The volume of  
165 the sample block varied with water content and was estimated using its dimensions at a  
166 number of points during the drying process.



167 All sensor output signals were logged with a CR10X datalogger (Campbell  
 168 Scientific, Inc.). TDR waveforms were analyzed with a computer algorithm based on  
 169 Heimovaara and Bouten (1990), but including an endpoint determination algorithm that  
 170 accounts for signal attenuation with increased travel time. All waveforms were analyzed  
 171 visually, following the recommendations of Dasberg and Hopmans (1992). The Vitel  
 172 sensor outputs three voltages for soil water content determination and one for sensor head  
 173 temperature, so that temperature compensation to dielectric and conductivity values can  
 174 be performed. The manufacturer provides an algorithm for this compensation. The CS615  
 175 sensor outputs a single period measurement from which the bulk soil dielectric constant  
 176 may be calculated using an empirical polynomial calibration. The manufacturer-supplied  
 177 calibrations are for  $20 \pm C$  and a correction coefficient has been developed for  
 178 measurement temperatures of 10 to  $30 \pm C$  (Campbell Scientific, Inc., 1996). Output from  
 179 the ECH<sub>2</sub>O (single voltage), GroPoint (single current) and Watermark (single resistance)  
 180 sensors were left untreated.

181 For TDR, the measured travel time of the is related to the permittivity:

$$182 \quad t > \frac{L\sqrt{\phi}}{c}$$

183 where  $t$  is the travel time,  $\phi$  is the relative dielectric permittivity,  $L$  is the length of the  
 184 TDR wave guides and  $c$  is the speed of light in free space ( $2.997 \times 10^8 \text{ m s}^{-1}$ ). For the  
 185 CS615 sensor, the measured response is a period from which the bulk dielectric constant  
 186 may be calculated:

$$187 \quad v > 2 \left( t_{cir}, \frac{2L\sqrt{e}}{c} \right)$$

188 where  $\nu$  is the period output,  $t_{cir}$  is delay of the circuit components,  $L$  is the probe length,  
 189  $c$  is the speed of light. The Vitel Hydraprobe is delivered with binary versions of  
 190 proprietary software that calculates soil water content from 3 sensor output voltages and  
 191 sensor temperature from the fourth voltage. Output values include the real and imaginary  
 192 parts of the soil dielectric constant, the soil conductivity, water content and temperature.  
 193 We make the assumption that the sensor response is accurately represented by the  
 194 calculated real part of the dielectric constant before temperature correction. The Delta-t  
 195 Theta probe operation has been described by Miller and Gaskin (1999). The measured  
 196 quantity for the sensor in a datalogging mode is a voltage for which Delta-t provides a  
 197 linear and a cubic calibration to relative dielectric permittivity:

$$198 \quad \sqrt{\phi} > 4.44V, 1.10$$

199 and:

$$200 \quad \sqrt{\phi} > 4.70V^3 + 6.40V^2, 6.40V, 1.07$$

201 where  $V$  is the sensor output voltage. The linear relationship is used for calibrations  
 202 relating the dielectric constant and volumetric water content. Similarly, the ECH<sub>2</sub>O form  
 203 of the empirical calibration suggested by the manufacturer is a linear relationship  
 204 between sensor output voltage and volumetric water content. GroPoint sensors are not  
 205 delivered with an algorithm for calculating dielectric constant from sensor output, but a  
 206 linear function is applied to the current output of the device.

207

## 208 **RESULTS AND DISCUSSION**

### 209 **Calibrations**

210 For all probes, excepting the Watermark, calibration curves were generated relating the  
211 gravimetrically-determined volumetric water content to sensor output over a range of  
212  $0.025 - 0.15 \text{ m}^3 \text{ m}^{-3}$  for live moss tissue and from  $0.025 - 0.20 \text{ m}^3 \text{ m}^{-3}$  for dead moss  
213 tissue. Figure 2 shows these results except for the Watermark sensor. The given  
214 volumetric water contents range from near field capacity to air-dry values. The field  
215 capacities for the live, dead and burnt mosses were approximately  $0.15$ ,  $0.20$  and  $0.20 \text{ m}^3$   
216  $\text{m}^{-3}$ , respectively. The rapid change in water content on removal of the sample block from  
217 the water hampered the determination of field capacity and of the bulk dielectric at water  
218 contents near field capacity. In practice, the field capacity depends on the nature of the  
219 underlying material. Least squares 2<sup>nd</sup> or 3<sup>rd</sup> order polynomial fits of the data for each of  
220 the sensors, excepting the Watermark, were performed. The polynomial coefficients and  
221 correlation coefficients are listed in Table 3, along with the probe output domain,  
222 expressed as a range of dielectric constant or sensor output values, for each relationship.

223 The Watermark sensor output decreased measurably up to volumetric water  
224 contents of 5% and 7% for live and dead moss, respectively. At higher water contents, the  
225 probe output is essentially independent of changes in water content. The Watermark  
226 probe distinguishes between the air-dry and near-saturated states of the moss.

227 The differences between sensor outputs under similar dielectric constant  
228 conditions suggest that the volume of sensitivity, which is the volume of bulk sample  
229 over which the probe measures a spatially weighted average dielectric constant, and  
230 spatial weighting within this volume, affected sensor output. For all of the sensors,  
231 sample volume proximal to the sensor tines is heavily weighted. Sensor insertion into the  
232 sample displaces moss. In contrast to mineral soil matrices, compression of the moss

233 around the sensor causes a localized increase in bulk density proximal to the sensor tines.  
234 Although the range of tine diameters for the sensors presented here is small (2.5 to 6  
235 mm), this effect would to an underestimate of water content increasing with tine  
236 diameter. Ferré (1996) showed that such effects are not independent of tine spacing,  
237 diameter and coating and of heterogeneities in the distribution of water around the sensor  
238 itself. Sensor dimensions play a larger role in moss than in mineral soils due to probe  
239 contact and air void effects, particularly for sensors using lower measurement frequencies  
240 than TDR, at which the apparent dielectric permittivity is more sensitive to bulk density  
241 (Hallikainen et al., 1985).

242         The question facing someone using any of these sensors in moss is what sort of  
243 calibration is necessary and sufficient to achieve a particular uncertainty. One can choose  
244 between calibrating for the specific material into which the sensor is to be installed,  
245 which is appropriate to permanent installation in a particular soil horizon. If the sensor is  
246 to be used in a handheld fashion in the field inserted from the surface, however, a wider  
247 range of materials will need to be included in the calibration. Based on the data presented  
248 here, we recommend separate calibrations for live and dead horizons, i.e. for differing  
249 stages of decomposition.

250         The feathermoss TDR calibrations presented here lie within the range of the low  
251 bulk density and organic media calibrations listed in the Introduction. The TDR graph of  
252 Figure 2 includes data for a block of charred dead feathermoss. This sample was dark,  
253 brittle and dusty, with a bulk density of over  $0.12 \text{ kg m}^{-3}$  for a 10 l sample. The TDR  
254 calibration curves suggests that burning feathermoss changes the apparent dielectric  
255 constant of the moss, presumably as a result of changes in the moss structure and perhaps

256 the formation of carbon deposits. In this study, live and dead moss output values  
257 approached each other at low water contents, but diverged with increasing water content.  
258 Probe output, or measured dielectric constant, was lower for live feathermoss than for  
259 dead at most volumetric water contents, for all tested probes except the ECH<sub>2</sub>O and the  
260 GroPoint sensors, for which sensor output values for live and dead moss were closer than  
261  $\pm 6\%$  (20 mV). This is generally consistent with the difference in bulk densities (live  
262  $0.022$ ; dead  $0.06 \text{ kg m}^{-3}$ ) observed.

263

## 264 **RECOMMENDATIONS**

265 We present calibration curves for six sensors in live and dead feathermoss. For all six,  
266 calibration curves for the calculation of volumetric water content from measured  
267 dielectric constant or sensor output, depending on sensor type, were created in live and  
268 dead feathermoss over a volumetric water content range of approximately  $0.02$  to  $0.2 \text{ m}^3$   
269  $\text{m}^{-3}$ . Calibration in multiple samples of the medium in which each sensor is to be used is  
270 advocated, whereby the uncertainty in the calibration is probably affected by spatial  
271 variability of the moss bulk density. The selection of samples for calibration should be  
272 determined by the intended use of the sensor. Sensor output in live and dead feathermoss  
273 layers at the same volumetric water content differ by more than 10% measured water  
274 content. Site-specific calibrations must therefore also record the horizons in which the  
275 sensors are being used, a consideration relevant to measurements made from the ground  
276 surface.

277

## 278 **ACKNOWLEDGEMENTS**

279 This research was supported by the National Science Foundation (OPP-9814835) and an  
280 Inland Northwest Research Alliance fellowship to the first author. We thank Martin  
281 Wilmking and Quinton Costello (University of Alaska Fairbanks) for their help with the  
282 laboratory experiment.

283

283 **REFERENCES**

- 284 Campbell Scientific, Inc. 1996. CS615 Water Content Reflectometer Instruction Manual,  
285 Version 8221-07. Campbell Scientific, Inc., Edmonton, Canada.
- 286 Dasberg, S., and Hopmans, J. W. 1992. Time domain reflectometry calibration for  
287 uniformly and nonuniformly wetted sandy and clayey loam soils. *Soil Sci. Soc.*  
288 *Am. J.* 56: 1341-1345.
- 289 Ferré, P. A., Rudolph, D. L., Kachanoski, R. G., 1996. Spatial averaging of water content  
290 by time domain reflectometry: Implications for twin rod probes with and without  
291 dielectric coatings. *Water Res. Res.* 32(2): 271-279.
- 292 Gray, A. N., and Spies, T. A. 1995. Water content measurement in forest soils and  
293 decayed wood using time domain reflectometry. *Can. J. For. Res.* 25: 376-385.
- 294 Hallikainen, M. T., Ulaby, F. T., Dobson, M. C., El-Rayes, M. A., and Wu, L.-K. 1985.  
295 Microwave dielectric behavior of wet soil – Part I: Empirical models and  
296 experimental observations. *IEEE Trans. Geosci. Remote Sensing.* GE-23(1): 25-  
297 34.
- 298 Harden, J.W., Neff, J.C., Sandberg, D.V., and Gleixner, G. 2004. Chemistry of burning  
299 the forest floor during the FROSTFIRE experimental burn, interior Alaska, 1999.  
300 *Glob. Biogeochem. Cycles* 18, doi:10.1029/2003GB002194.
- 301 Heimovaara, T. J., and Bouten, W. 1990. A computer-controlled 36-channel time domain  
302 reflectometry system for monitoring soil water contents. *Water Resour. Res.*,  
303 26(10): 2311-2316.

- 304 Herkelrath, W. N., Hamburg, S. P., and Murphy, F. 1991. Automatic, real-time  
305 monitoring of soil moisture in a remote field area with time domain reflectometry.  
306 *Water Resour. Res.* 27(5):857-864.
- 307 Hinkel, K. M., R. F. Paetzold, F. E. Nelson, and J. G. Bockheim, 2001. Patterns of soil  
308 temperature and moisture in the active layer and upper permafrost at Barrow,  
309 Alaska: 1993–1999. *Global Planet. Change*, 29: 293 –309.
- 310 Jacobsen, O. H., and Schønning, P. 1995. Proceedings of the symposium: time domain  
311 reflectometry applications in soil science. SP Rapport (0908-2581) nr. 11, pp. 25-  
312 33.
- 313 Kane, D. L., Seifert, R. D., and Taylor, G. S. 1978. Hydrologic properties of subarctic  
314 organic soils. U.S. Forest Service, Institute of Northern Forestry, Report No.  
315 IWR-88.
- 316 King, S., Harden, J.W., Manies, K.L., Munster, J., and White, L.D. 2002. Fate of carbon  
317 in Alaskan landscape project - database for soils from eddy covariance tower  
318 sites, Delta Junction, AK. U.S. Geological Survey Open File Report 02-62. 45  
319 pages.
- 320 Knight, J. H. 1992. The sensitivity of time domain reflectometry measurements to lateral  
321 variations in soil water content. *Water Resour. Res.* 28: 2345–2352.
- 322 Ledieu, J., Ridder, P. de, Clerck, P. de, and Dautrebande, S. 1986. A method of  
323 measuring soil moisture by time-domain reflectometry. *J. Hydrol.* 88:319-328.
- 324 Malicki, M. A., and Skierucha, W. M. 1989. A manually controlled TDR soil moisture  
325 meter operating with 300 ps rise-time needle pulse. *Irrigation Science*, 10: 153-  
326 163.



- 327 Manies, K.L. and Harden, J.W. 2004. Soil data from *Picea mariana* stands near Delta  
328 Junction, AK of different ages and soil drainage type. U.S. Geological Survey  
329 Open File Report 2004-1271. 19 pp.
- 330 Miller, J. D. and Gaskin, G. J. 1999. ThetaProbe ML2x: Principles of operation and  
331 applications. Macaulay Land Use Research Institute Technical Note (2nd ed.),  
332 Aberdeen, Scotland.
- 333 Myllys, M., and Simojoki, A. 1996. Calibration of time domain reflectometry (TDR) for  
334 soil moisture measurements in cultivated peat soils. *Suo* 47(1): 1-6.
- 335 Nadler, A., Dasberg, S., and Lapid, I. 1991. Time domain reflectometry measurements of  
336 water content and electrical conductivity of layered soil columns. *Soil Sci. Soc.*  
337 *Am. J.* 55: 938-943.
- 338 Nissen, H. H., Ferre, P. A., and Moldrup, P. 2003. Metal-coated printed circuit board time  
339 domain reflectometry probes for measuring water and solute transport in soil.  
340 *Water Resour. Res.* 39(7): 1184.
- 341 O'Neill, K.P., Harden, J.W., and Trumbore, S.E. 1995. Boreal-ecosystem atmosphere  
342 study (BOREAS): 1993 laboratory data and notes: Thompson, Manitoba. USGS  
343 Open File Report 95-488.
- 344 Or, D., and Wraith, J. M. 1999. Temperature effects on soil bulk dielectric permittivity  
345 measured by time domain reflectometry: a physical model. *Water Resour. Res.*  
346 35(2): 371-383.
- 347 Pepin, S., Plamondon, A. P., and Stein J. 1992. Peat water content measurement using  
348 time domain reflectometry. *Can. J. For. Res.* 22: 532-540

- 349 Romanovsky, V. E., Osterkamp, T. E. 2000. Effects of unfrozen water on heat and mass  
350 transport processes in the active layer and permafrost. *Permafrost and Periglac.*  
351 *Process.* 11: 219-239.
- 352 Roth, K., Schulin, R., Fluehler, H., and Attinger, W. 1990. Calibration of time domain  
353 reflectometry for water content measurement using a composite dielectric  
354 approach. *Water Resour. Res.* 26: 2267-2273.
- 355 Roth, C. H., Malicki, M.A., and Plagge, R.1992. Empirical evaluation of the relationship  
356 between soil dielectric constant and volumetric water content as the basis for  
357 calibrating soil moisture measurements by TDR. *J. Soil Sci.* 43:1-13.
- 358 Schaap, M. G., Lange, L. D., and Heimovaara, T. J. 1996. TDR calibration of the organic  
359 forest floor material. *Soil Technology* 11: 205-217.
- 360 Stein, J., and Kane, D. L. 1983. Monitoring the unfrozen water content of soil and snow  
361 using time domain reflectometry. *Water Resour. Res.* 19: 1573-1584.
- 362 Toikka, M. V., and Hallikainen, M. 1989. A practical electric instrument for *in situ*  
363 measurements of peat properties. In: Dodd, V. A., Grace, P. M. (eds) *Land and*  
364 *Water Use*, pp. 101-105, Balkema, Rottersdam.
- 365 Topp, G. C., Davis, J. L. and Annan, A. P. 1980. Electromagnetic determination of soil  
366 water content: measurements in coaxial transmission lines, *Water Resour. Res.*  
367 16: 574-582.
- 368 Trumbore, S.E., Bubier, J. Harden, J.W., and Crill, P.M. 1999. Carbon cycling in boreal  
369 wetlands: a comparison of three approaches. *J. Geophys. Res. Atmos.* 104: 27  
370 673-27 682.

- 371 Wraith, J. M., and Or, D. 1999. Temperature effects on soil bulk dielectric permittivity  
372 measured by time domain reflectometry: experimental evidence and hypothesis  
373 development. *Water Resour. Res.* 35(2): 361-369.
- 374 Yoshikawa, K., Bolton, W. R., Romanovsky, V. E., Fukuda, M., and Hinzman, L. D.  
375 2003. Impacts of wildfire on the permafrost in the boreal forests of interior  
376 Alaska. *J. Geophys. Res.* 108(D1).
- 377 Yoshikawa, K., Overduin, P. P., and Harden, J. 2004 (in press). Moisture content  
378 measurements of moss (*Sphagnum* spp.) layers using recently developed sensors.  
379 *Permafrost and Periglacial Processes*.
- 380 Zegelin, S. J., White, I., and Jenkins, D. R. 1989. Improved field probes for soil water  
381 content and electrical conductivity measurement using time domain reflectometry.  
382 *Water Resour. Res.* 25(11): 2367-2376.
- 383

383 **List of Tables**

384 **Table 1.** Bulk density ranges for feather and *Sphagnum* mosses from the literature.

385 **Table 2.** The physical and operating characteristics of the sensors.

386 **Table 3.** Calibration coefficients for relating sensor output or measured dielectric to

387 volumetric water content in live and dead feathermoss. The coefficients for the

388 expression:

389 
$$\text{volumetric water content} = a x + b,$$

390 are given, where x is either sensor output or the square root of the dielectric constant, as

391 listed in Table 2. The range of sensor output or dielectric constant for which the sensors

392 were calibrated in feathermoss is given the rightmost columns (units are listed in Table

393 2).

394 **List of Figures**

395 **Figure 1.** Bulk density as a function of depth for live and dead feathermoss layers from  
396 Delta Junction, Alaska - Manies et al.; Manitoba, Canada - O'Neill et al., (1995) and the  
397 Frostfire experiment in Alaska - Harden et al., (2004).

398 **Figure 2.** Variation in measured dielectric constant (CS615, TDR, Theta and Vitel  
399 sensors) or sensor output (ECH<sub>2</sub>O and GroPoint) with volumetric soil water content for  
400 six sensors for live and dead feathermoss. The TDR graph shows additional data from a  
401 sample of charred feathermoss.

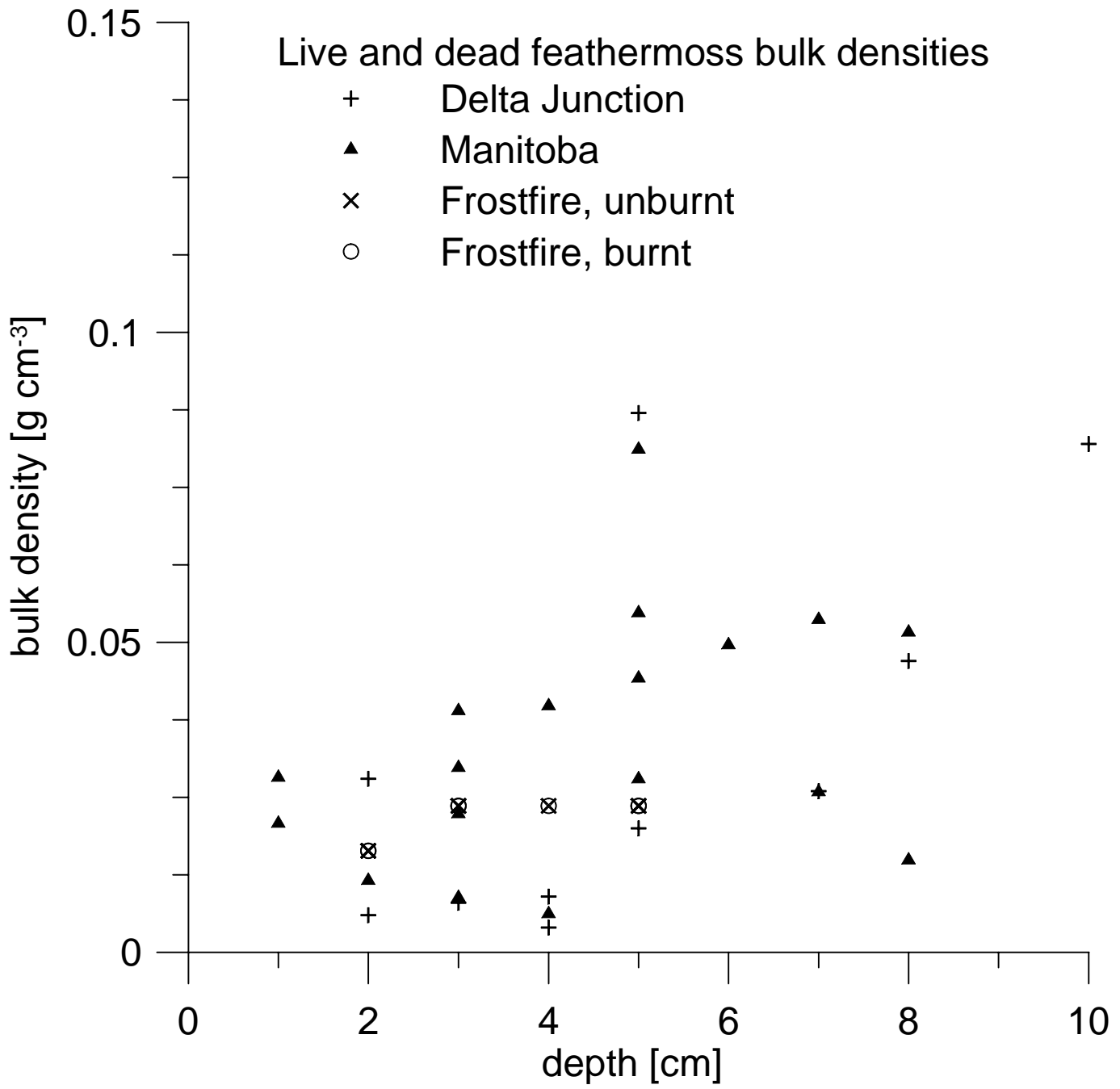
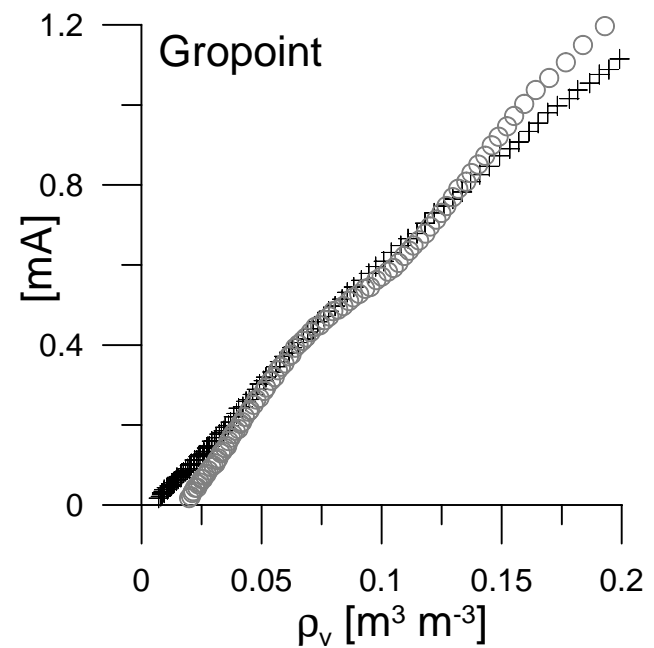
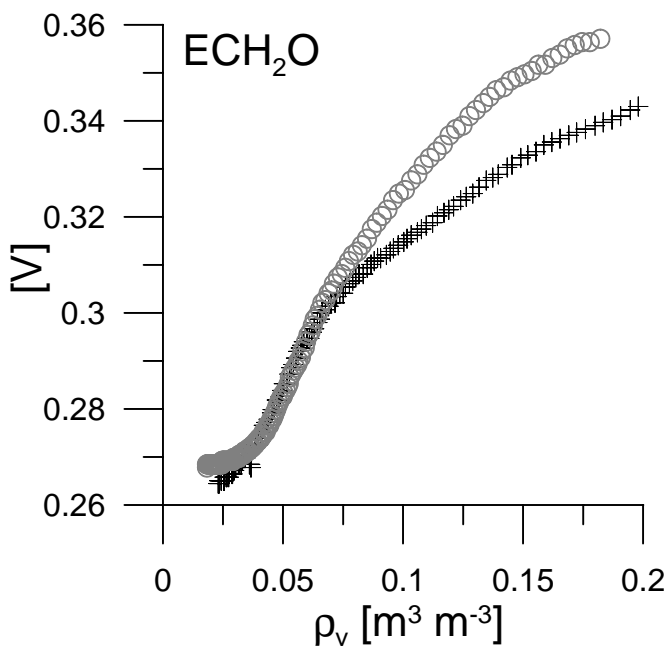
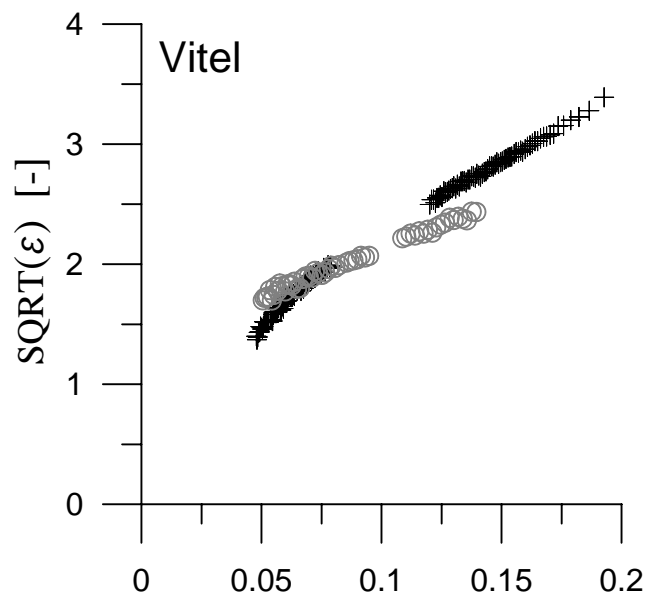
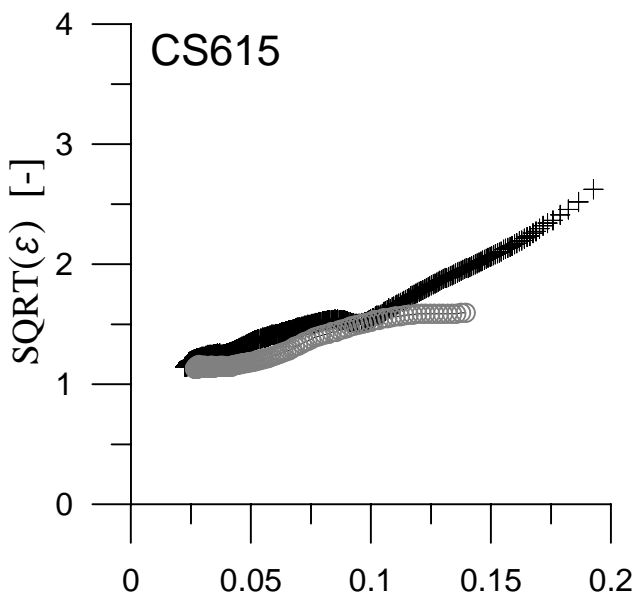
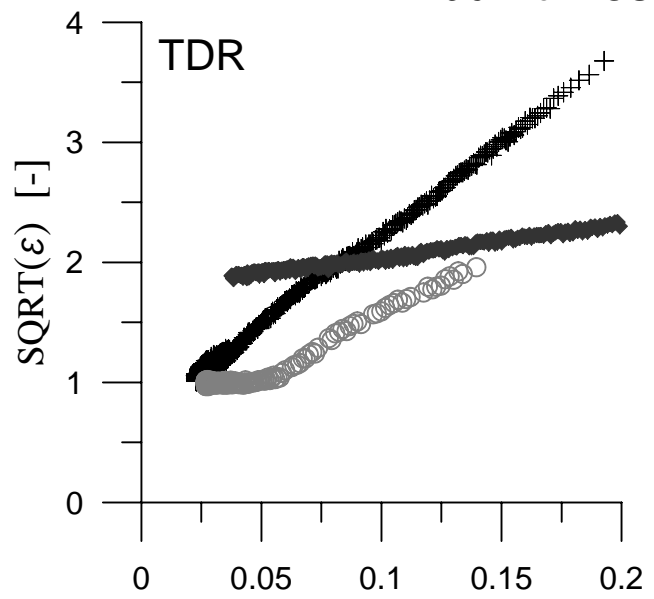
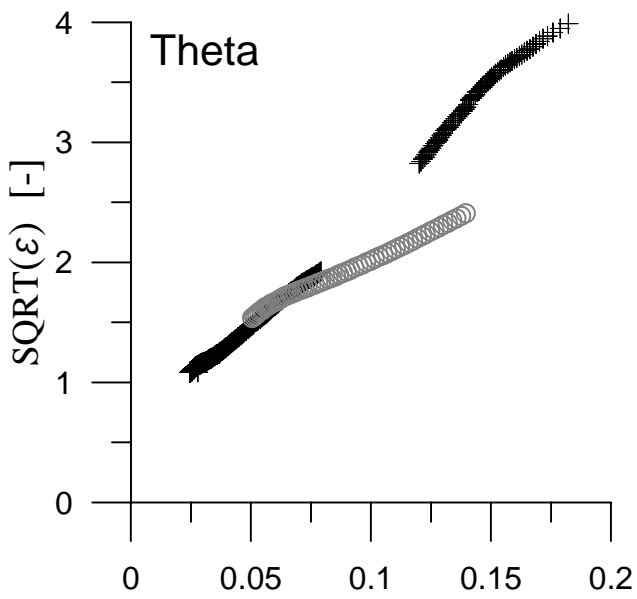


Figure 1.

# Feather Moss

- + dead moss
- live moss
- ◆ burnt moss



sample	Bulk density [ $\text{kg m}^{-3}$ ]	
	live (# samples)	dead (# samples)
Feather moss species dry bulk density	0.013 (6) <sup>†</sup>	0.049 (6) <sup>†</sup>
	0.019 (6) <sup>‡</sup>	0.041 (8) <sup>‡</sup>
	0.040 (27) <sup>§</sup>	0.092 (7) <sup>§</sup>
	0.022 (23) <sup>¶</sup>	0.06 (1) <sup>¶</sup>
Sphagnum moss species dry bulk density	---	0.108 <sup>#</sup>
	---	0.8 – 100 <sup>‡‡</sup>
	0.0129 - 0.0314 <sup>§§</sup>	
	0.0168 - 0.0406 <sup>§§</sup> (capitulum)	
	0.019 – 1.40 (corresponding to mat thicknesses of 3 – 47 cm) <sup>§§</sup>	

† – Trumbore et al. (1999); ‡ – King et al. (2002);  
§ – O'Neill et al. (1995); ¶ – this study; # –  
Yoshikawa et al. (2004); ‡‡ – Yoshikawa et al.  
(2003); §§ – Kane et al. (1978).

Table 1.



type	Sensor	Characteristics			Dimensions [mm]		
		frequency [MHz]	wave shape	sensor output	sensor length	tine diameter	tine spacing (#)
Time Domain	<b>CS615</b>	55.5	sine	<b>1 pulse</b> [700 - 1400 ms]	288	3.2	28.5 (2)
	<b>GroPoint</b>	2 (0.5 microns)	pulse	<b>1 current</b> [0-5 mA]	205	6	25 (2)
	<b>TDR100</b>	3000 (130 ps)	pulse	<b>waveform</b> voltage vs. time	300	4.8	22 (3)
Frequency Domain	<b>ECH<sub>2</sub>O</b>	2 (pulse)/6 (sine)	pulse/sine	<b>1 voltage</b> [400-1000 mV]	200	2.5/7.5	6 (3)
	<b>Theta</b>	100 MHz	sine	<b>1 voltage</b> [<1000 mV]	59	3.2	10 (2)
	<b>Vitel</b>	50 MHz	sine	<b>4 voltages</b> [<2500 mV]	57	4	8.6 (4)
Electrical Resistance	<b>Watermark</b>	DC	---	<b>1 resistance</b> [0.1-500 kΩ]	70	22.5	---

Table 2.

sensor	moss	coefficients		output domain <sup>†</sup>		
		<i>a</i>	<i>b</i>	<b>R</b> <sup>2</sup>	<b>x</b> <sub>min</sub>	<b>x</b> <sub>max</sub>
<b>CS615</b>	dead	6.99 x 10 <sup>0</sup>	9.80 x 10 <sup>-1</sup>	0.981	1.18	1.58
	live	4.88 x 10 <sup>0</sup>	9.84 x 10 <sup>-1</sup>	0.966	1.14	2.63
<b>ECH<sub>2</sub>O</b>	dead	5.00 x 10 <sup>-1</sup>	2.58 x 10 <sup>-1</sup>	0.937	270	357
	live	6.58 x 10 <sup>-1</sup>	2.52 x 10 <sup>-1</sup>	0.975	264	384
<b>GroPoint</b>	dead	5.92 x 10 <sup>0</sup>	1.00 x 10 <sup>-2</sup>	0.996	0.02	1.70
	live	6.69 x 10 <sup>0</sup>	8.08 x 10 <sup>-2</sup>	0.994	0.02	1.55
<b>TDR</b>	dead	1.55 x 10 <sup>1</sup>	6.83 x 10 <sup>-1</sup>	0.997	1.04	1.96
	live	8.05 x 10 <sup>0</sup>	7.46 x 10 <sup>-1</sup>	0.929	1.02	3.67
	burnt	2.69 x 10 <sup>0</sup>	1.77 x 10 <sup>0</sup>	0.983	1.86	2.34
<b>Theta</b>	dead	1.90 x 10 <sup>1</sup>	5.80 x 10 <sup>-1</sup>	0.995	2.40	5.80
	live	9.22 x 10 <sup>0</sup>	1.10 x 10 <sup>0</sup>	0.998	1.18	16.8
<b>Vitel</b>	dead	1.31 x 10 <sup>1</sup>	8.98 x 10 <sup>-1</sup>	0.993	1.70	2.43
	live	8.05 x 10 <sup>0</sup>	1.32 x 10 <sup>0</sup>	0.989	1.37	3.39

<sup>†</sup> – sensor outputs and units are listed in Table 2.

Table 3.